DEPARTMENT OF THE INTERIOR
U.S. GEOLOGICAL SURVEY

Prepared for the
NATIONAL AERONAUTICS AND SPACE ADMINISTRATION

ATLAS OF MERCURY
1:5,000,000 GEOLOGIC SERIES
BOREALIS REGION
H 5M 90/0 G, 1984
I-1660 (H-1)

NOTES ON BASE

This map sheet is one of a series covering that part of the surface of Mercury that was illuminated during the Mariner 10 encounters (Davies and Batson, 1975). The source of map data was the Mariner 10 television experiment (Murray, 1975).

ADOPTED FIGURE

The map projections are based on a sphere with a radius of 2439 km.

PROJECTION

The polar stereographic projection is used for this sheet, with a scale of 1:4,290,000 at lat 65°. Latitudes are based on the assumption that the spin axis of Mercury is perpendicular to the plane of the orbit. Longitudes are positive westward in accordance with the usage of the International Astronomical Union (IAU, 1971). Meridians are numbered so that a reference crater named Hun Kal (lat 0.6° S.) is centered on long 20° (Murray and others, 1974; Davies and Batson, 1975).

CONTROL

Planimetric control is provided by photogrammetric triangulation using Mariner 10 pictures (Davies and Batson, 1975). Discrepancies between images in the base mosaic and computed control-point positions appear to be less than 2 km, except for the area east of about long 90°. Pictures of this area are so foreshortened that accurate map transformations were not possible. Since the base mosaic was controlled by a later iteration of the control net, discrepancies as large as 20 km exist between this sheet and the Victoria (H-2) and Shakespeare (H-3) sheets to the south. These discrepancies were adjusted within the area north of lat 70°.

MAPPING TECHNIQUES

Mapping techniques are similar to those described by Batson (1973a, 1973b). A mosaic was made with pictures that had been digitally transformed to the polar stereographic projection. Shaded relief was copied from the mosaics and portrayed with uniform illumination with the sun to the west. Many Mariner 10 pictures besides those in the base mosaic were examined to improve the portrayal. The shading is not generalized and may be interpreted with nearly photographic reliability (Inge, 1972; Inge and Bridges, 1976).

Shaded relief analysis and representation were made by J. L. Inge.

NOMENCLATURE

All names on this sheet are approved by the International Astronomical Union (IAU, 1977).

H-1: Abbreviation for Mercury (Hermes) sheet number 1.

H 5M 90/0 G: Abbreviation for Mercury (Hermes) 1:5,000,000 series; center of sheet, lat 90° N., long 0°; geologic map, G.

REFERENCES

Batson, R. M., 1973a, Cartographic products from the Mariner 9 mission: Journal of Geophysical Research, v. 78, no. 20, p. 4424-4435.
———1973b, Television cartography: U.S. Geological Survey open-file report, Astrogeology 58, 35 p.
Davies, M. E., and Batson, R. M., 1975, Surface coordinates and cartography of Mercury: Journal of Geophysical Research, v. 80, no. 17, p. 2417-2430.
Inge, J. L., 1972, Principles of lunar illustration: Aeronautical Chart and Information Center Reference Publication RP-72-1, 60 p.
Inge, J. L., and Bridges, P. M., 1976, Applied Photointerpretation for airbrush cartography: Photogrammetric Engineering and Remote Sensing, v. 42, no. 6, p. 749-760.
International Astronomical Union, 1971, Commission 16: Physical study of planets and satellites, *in* 14th General Assembly, Brighton, 1970, Proceedings: International Astronomical Union Transactions, v. 14B, p. 105-108.
———1977, Working Group for Planetary System Nomenclature, *in* 16th General Assembly, Grenoble, 1976, Proceedings: International Astronomical Union Transactions, v. 16B, p. 321-325, 330-332, 351-355.
Murray, B. C., 1975, The Mariner 10 pictures of Mercury—an overview: Journal of Geophysical Research, v. 80, no. 17, p. 2342-2344.
Murray, B. C., Belton, M. J. S., Danielson, G. E., Davies, M. E., Gault, D. E., Hapke, Bruce, O'Leary, Brian, Strom, R. G., Soumi, Verner, and Trask, Newell, 1974, Mercury's surface: Preliminary description and interpretation from Mariner 10 pictures: Science, v. 185, no. 4146, p. 169-179.

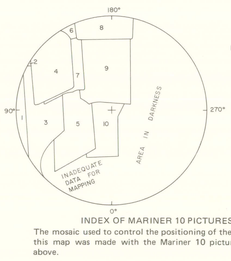

Index No.	FDS No.
1	148
2	149
3	152
4	157
5	160
6	162
7	161
8	166
9	165
10	164

INDEX OF MARINER 10 PICTURES

The mosaic used to control the positioning of the features on this map was made with the Mariner 10 pictures outlined above.

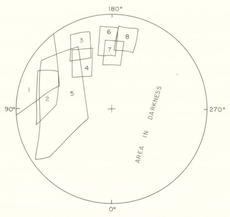

Index No.	FDS No.
1	153
2	83
3	88
4	84
5	156
6	87
7	83
8	86

SUPPLEMENTAL SOURCE INDEX

The Mariner 10 pictures outlined above were used to provide additional detail on the map but were not used on the controlled mosaic.

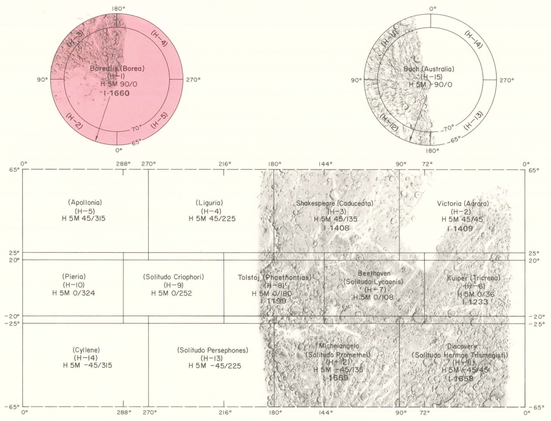

ARRANGEMENT OF MAP SHEETS ON MERCURY

The provisional name "Goethe" was changed to "Borealis," and the provisional name "Tir" was changed to "Tolstoj" by the International Astronomical Union in 1976 (IAU, 1977). These provisional names appeared on earlier editions of this index map and on the shaded relief map of the Tolstoj (H-8) quadrangle. The number preceded by I refers to published geologic map.

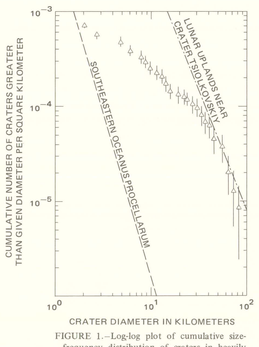

FIGURE 1.—Log-log plot of cumulative size-frequency distribution of craters in heavily cratered intercrater plains material in the Borealis region within a belt bordering terminator and within an east-facing area east of crater Jókai. Note decrease in slope of the Mercurian curve where craters are smaller than 30 km and larger than 60 km. Also note coincidence of the abundance of craters 10 to 55 to 65-km-diameter range with the curve for lunar pre-Nectarian terra northwest of crater Tsiolkovskiy. Intercrater plains material has been more heavily impacted by craters larger than 4 km in diameter (and is, therefore, older) than southeastern part of Oceanus Procellarum, the near-average lunar mare. (See section on stratigraphy.) Bars represent standard error or deviation ($\pm\sqrt{N}/A$; where N=cumulative number of craters greater than given diameter per square kilometer and A=unit area). Crater counts and curves by Arthur L. Dial, Jr.

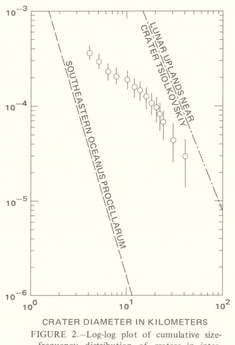

FIGURE 2.—Log-log plot of cumulative size-frequency distribution of craters in intermediate plains material within and adjoining the Borealis region. Crater density is intermediate between those of intercrater plains and smooth plains materials. (For explanation of lunar curves, see fig. 1 and section on stratigraphy.) Bars represent standard error or deviation ($\pm\sqrt{N}/A$; where N=cumulative number of craters greater than given diameter per square kilometer and A=unit area). Crater counts and curves by Arthur L. Dial, Jr.

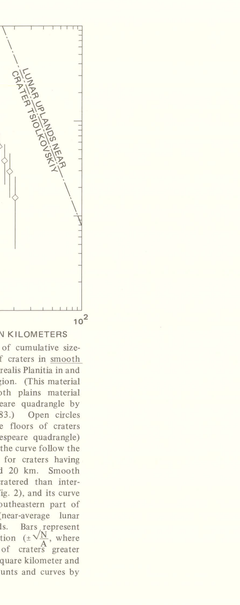

FIGURE 3.—Log-log plot of cumulative size-frequency distribution of craters in smooth plains material of Borealis Planitia in and adjoining the Borealis region. (This material includes the very smooth plains material mapped in the Shakespeare quadrangle by Guest and Greeley, 1983.) Open circles represent counts on the floors of craters Strindberg (in the Shakespeare quadrangle) and Turgenev. Note that the curve follow the -2 distribution function for craters having diameters between 3 and 20 km. Smooth plains material is less cratered than intermediate plains material (fig. 2), and its curve lies between those of southeastern part of Oceanus Procellarum (near-average lunar mare) and lunar uplands. Bars represent standard error or deviation ($\pm\sqrt{N}/A$; where N=cumulative number of craters greater than given diameter per square kilometer and A=unit area). Crater counts and curves by Arthur L. Dial, Jr.

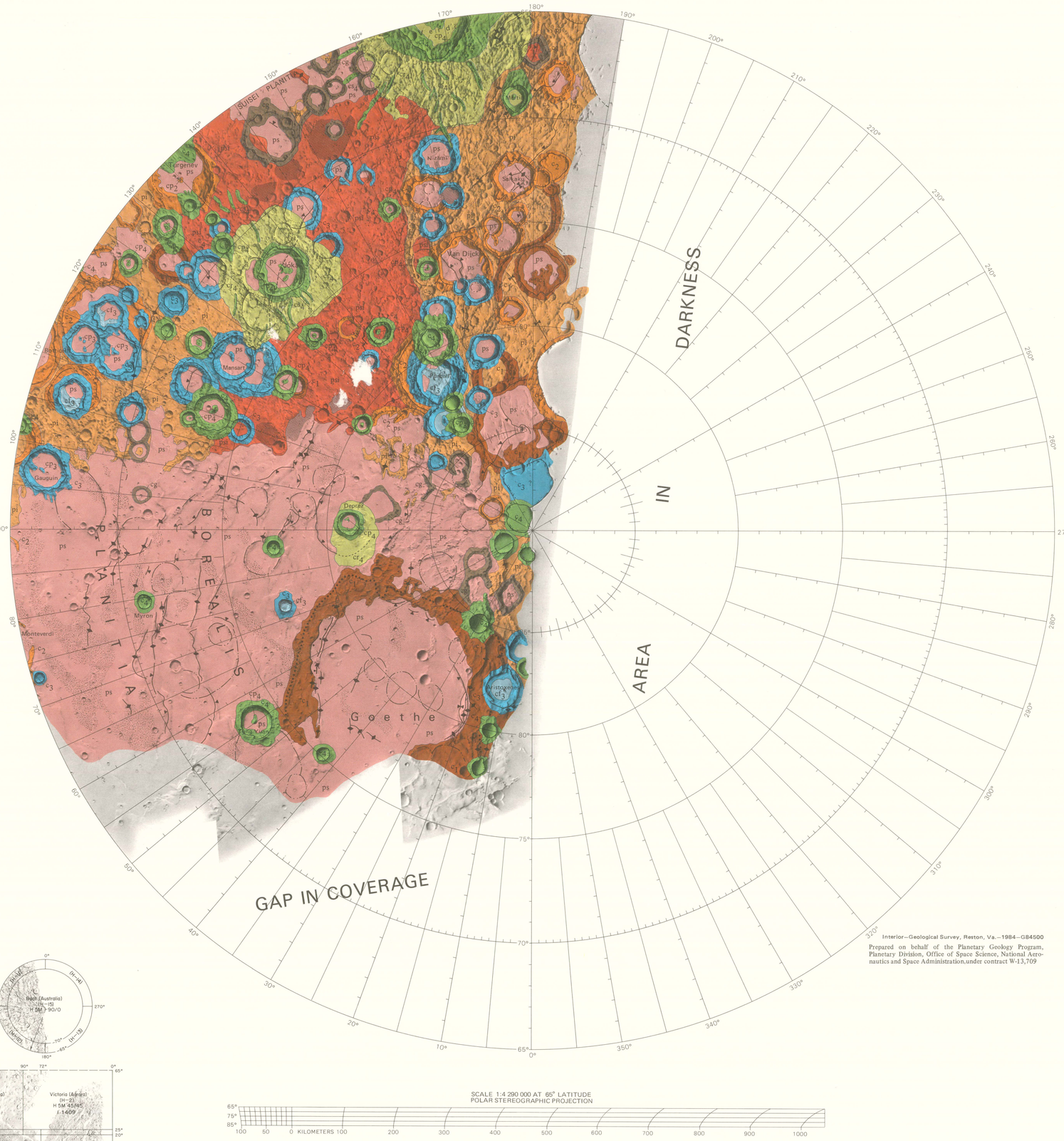

Interior—Geological Survey, Reston, Va.—1984—G84500

Prepared on behalf of the Planetary Geology Program, Planetary Division, Office of Space Science, National Aeronautics and Space Administration, under contract W-13,709

SCALE 1:4 290 000 AT 65° LATITUDE
POLAR STEREOGRAPHIC PROJECTION

65° 75° 85°

100 50 0 KILOMETERS 100 200 300 400 500 600 700 800 900 1000

CORRELATION OF MAP UNITS

PLAINS MATERIAL	BASIN AND CRATER MATERIALS				
ps		c_4	cp_4	cf_4	cr_4	cs_4
psi	Caloris event	c_3	cp_3	cf_3		cg
pi		c_2	cp_2			
	Goethe event	c_1				

DESCRIPTION OF MAP UNITS

PLAINS MATERIALS

ps — SMOOTH PLAINS MATERIAL–Forms flat to gently rolling plains at resolution of Mariner 10; commonly occurs in low depressions such as Borealis and Suisei Planitiae, in basins such as Goethe (FDS 160), and in large c_1 to c_4 craters (FDS 156). Intermediate albedo. Characterized by sharp or gradational overlapping contacts with older terrain and by sparsity of c_1 to c_3 craters, except for subjacent ghost craters. Sinuous ridges and scarps common. *Interpretation:* Probably lava; no volcanic vents observed. Two very long but discontinuous scarps concentric to Goethe Basin and one circular scarp bounding shieldlike platform around crater Deprez may represent fronts of viscous volcanic lava flows that crossed Borealis Planitia. Alternatively, may consist of fluidized shock-melted material

psi — INTERMEDIATE PLAINS MATERIAL–Forms flat to gently rolling plains north and northeast of Suisei Planitia (FDS 157, 161). Albedo similar to that of smooth plains material. Contains fewer superposed craters than intercrater plains material and more than smooth plains material. Embayment relations with older and younger plains materials unclear, except along western border of Borealis Planitia. *Interpretation:* Uncertain: may consist of impact materials ranging from basin and crater ejecta, similar to some facies in Caloris Basin ejecta, to shock melt and breccia; may also consist in part of volcanic materials. Intermediate crater density may indicate age transitional between intercrater plains and smooth plains materials

pi — INTERCRATER PLAINS MATERIAL–Forms hummocky, pitted, locally grooved and lineated plains mostly west of the 100° meridian (FDS 152, 165). Albedo similar to that of smooth plains and intermediate plains materials. High density of superposed, overlapping craters 5 to 10 km in diameter; most craters elliptical, shallow, and open on one side, superposed on degraded remnants of larger craters. Unit overlaps or overlies rounded rims of ghost craters in Suisei Planitia and north of Goethe Basin. *Interpretation:* May be mixture of basin and crater ejecta and volcanic deposits emplaced during terminal phase of heavy bombardment

BASIN AND CRATER MATERIALS

c_4 — CRATER MATERIALS–Craters >30 km in diameter showing various degrees of degradation and burial. Subscripts refer to degradation sequence from c_1 (most degraded) to c_4 (least degraded). *Interpretation:* Formed by impact. Degree of degradation is assumed to represent relative age (c_1 oldest to c_4 youngest) of craters of closely similar diameters (McCauley and others, 1981)

cp_4 — Material of craters with scalloped or slightly subdued rims, terraced walls, and terraces disrupted by slumping–Central peak or peaks usually present; sharp contact of wall with floor. *Interpretation:* Rim material consists of overturned flap and fallback; upper part of wall is bedrock; slump and colluvium along footwall and base of terraces. Floor consists of brecciated bedrock and fallback ejecta; floors partly flooded with smooth plains material representing impact melt or post-impact lava flows

cf_4 — Central peak material of c_4 craters–Peaks either single or more rarely in clusters of multiple peaks that rise above crater floors near their centers (Verdi, FDS 166; Jókai, FDS 161). *Interpretation:* Formed by rebound after impact

cr_4 — Crater floor material of c_4 craters–Material of some crater floors is hilly, hummocky, or rolling; other crater floors surfaced by smooth plains material. *Interpretation:* Hummocks are blocks of fallback ejecta; smooth surface represents resurfacing by shock melt or lava flows

cs_4 — Crater ejecta material, radial–Forms well-developed, radially lineated, distinctive annulus adjacent to rims of large c_4 craters. *Interpretation:* Ballistically emplaced ejecta, mixed with precrater material: the small-crater equivalent of lineated facies of Van Eyck Formation (McCauley and others, 1981) surrounding Caloris Basin

c_3 — Secondary crater material–Forms crater chains or clusters of small, fresh craters oriented radially to and generally related to primary craters Verdi and Jókai. Only a few major chains of secondary craters around Verdi and Jókai mapped. *Interpretation:* Nearby and farflung secondary ejecta from primary impacts

cp_3 — Material of craters with low, rounded, but continuous rims (FDS 156)–Floors flat, partly filled with smooth plains or intermediate plains materials. Wall terraces rare, but radial channels on wall common at Mansart; floor-wall boundary indistinct in many craters. Discontinuous field of secondary craters common. Moderate number of superposed craters

cf_3 — Central peak material of c_3 craters–Same as cp_4 except occurs within c_3 craters. Peaks either single or multiple

c_2 — Crater floor material of c_3 craters–Same as cf_4 except occurs within c_3 craters

cp_2 — Material of pan-shaped craters with low rims covered with superposed primary and secondary craters (FDS 165)–Degraded wall terraces. Crater floor flooded with intercrater plains and smooth plains materials. No visible secondary craters

c_1 — Central peak material of c_2 craters–Same as cp_3 and cp_4 except occurs in c_2 crater Turgenev

cg — Material of flat-floored craters with no central peak and with low, discontinuous rims (FDS 164)–No wall structure; no field of secondary craters. Crater floor flooded with smooth plains and intercrater plains materials. *Interpretation of units c_2 through c_1:* Materials of impact craters displaying various stages of degradation and infilling. Bimodal morphologic classification of craters >100 km and <100 km after McCauley and others (1981)

Material of ghost craters–Cannot be dated by usual sequence of degradation; rounded rims of intercrater plains material embayed by smooth plains material (FDS 162). Age may range from c_1 to late c_3. *Interpretation:* Material of crater rims, including overturned layers, primary and secondary crater ejecta, and superposed plains material

CONTACT–Dashed where approximately located; dotted where obliterated; queried where probable

FAULT–Bar and ball on downthrown side

LINEAMENT–Probably a fault with no vertical relief or a fault of uncertain displacement. May include unresolved crater chains of secondary-impact origin

NARROW TO BROAD RIDGE–Symbol on ridge crest. Interpreted within smooth plains material as mare-type wrinkle ridge

RIDGE SCARP, LINEAR TO ARCUATE–Line marks base of slope. Barb points downslope; dotted where concealed. Interpreted within smooth plains material as distal edge of lava flow

FISSURE OR TROUGH OF STRUCTURAL ORIGIN, LINEAR TO ARCUATE–Barbs point downslope

CRATER RIM CREST

CRATER RIM CREST, GREATLY SUBDUED OR BURIED–In Borealis Planitia and Goethe Basin, symbol represents ghost craters

CRESTLINE OF GOETHE BASIN–Much subdued, only approximately located

AREA OF BRIGHT CRATER-RAY MATERIAL–Interpreted as ejecta from very fresh impacts

AREA OF ANOMALOUSLY LOW ALBEDO

INTRODUCTION

The Borealis region surrounding the north pole of Mercury contains the Goethe Basin, whose diameter of at least 400 km makes it the sixth largest impact basin observed on Mariner 10 images (Murray and others, 1974; Strom and others, 1975; Trask and Guest, 1975; Boyce and Grolier, 1977; Strom, 1977, 1979). The west half of the mapped area (between long 100° and 190° W.) is dominated by older craters of c_1, c_2, and c_3 ages and by intercrater plains material that lies between and within them. Younger crater materials of c_4 age, intermediate plains material, and small patches of smooth plains material are superposed on all other units. The c_4 crater Verdi, 122 km in diameter, is the largest of the younger craters. Its extensive ejecta blanket and secondary crater field are superposed on plains materials and older craters.

The east half of the mapped area (between long 0° and 100° W.) is characterized by smooth plains material (Murray and others, 1974; Trask and Strom, 1976). This unit covers vast expanses of Borealis Planitia, a depression about 1,000 km in diameter that has an irregular arcuate west boundary. This depression is located over the site(s) of one or several old impact structures (Trask and Strom, 1976; Boyce and Grolier, 1977; Strom, 1979).

In the Borealis region, Mariner 10 images are available for only the western hemisphere, from long 0° to about long 190° W. Mercury was in darkness beyond long 190° W. on March 29, 1974, when the first Mariner 10 flyby acquired the most useful photographs of the region.

Most of the photographs used for geologic mapping were acquired by the departing spacecraft during the first pass (Mercury I). The Mercury II encounter provided no usable images of the map area; two low-oblique photographs suitable for geologic mapping were acquired during the third flyby on March 17, 1975 (Davies and others, 1978, p. 31). No stereoscopic photographic pairs are available for the Borealis region.

Because the terminator was a few degrees away from the 0°–180° meridian at the time of the first encounter, photographs of the region were acquired under a wide range of lighting conditions. These conditions and the large obliquity of the photographs hampered geologic interpretation of surface materials in the map area, as they did in the Kuiper (De Hon and others, 1981), Victoria (McGill and King, 1983), and Shakespeare (Guest and Greeley, 1983) quadrangles to the south.

Mercury's Equatorial plane is inclined less than 2° to its orbital plane (Klaasen, 1976; Murray and others, 1981, p. 28); its rotation period of 58.64 terrestrial days is in two-thirds resonance with its orbital period of 87.97 terrestrial days (Colombo, 1965; Colombo and Shapiro, 1966; Davies and others, 1978, p. 31). The resulting lag and orbital eccentricity create a variation of mean temperature not only with latitude, as on the Earth, but also with longitude. However, because of Mercury's relatively slow rotational peroid, diurnal variations in temperature probably greatly exceed mean-temperature variations along latitude and longitude, even in the high latitudes. Its pronounced orbital eccentricity (0.2563) causes the apparent solar intensity at Mercury to vary by more than a factor of 2 throughout a Mercurian year (Davies and others, 1978, p. 2), corresponding to about a 20 percent change in equilibrium temperature. Further, conservation of orbital angular momentum and spin-orbit coupling cause considerable variation in the length of daylight. Dawns and sunsets are prolonged by the long transit time of the Mercurian horizon across the sun disk; thus, daylight is lengthened and nightime reduced by several terrestrial days at sunset and vice versa at sunrise (Robert Wildey, U.S. Geological Survey, oral commun., 1982). Despite these considerations and despite the daily range in surface temperatures of several hundred degrees Kelvin, the subsurface temperature in the polar regions always remains well below freezing (Murray, 1975).

STRATIGRAPHY

Within the Borealis region, three widespread plains units are recognized largely by their obvious differences in crater density, which is closely related to relative age (Soderblom and Boyce, 1972). From most heavily cratered (oldest) to least cratered (youngest), these units are intercrater plains material (unit pi), intermediate plains material (unit psi), and smooth plains material (unit ps). Visual identification is confirmed and refined by actual crater counts (table 1). If we use the lunar surface as a frame of reference, the crater density of Mercurian plains in the Borealis region is bracketed by that of the lunar uplands, the most heavily cratered lunar surface, and that of Oceanus Procellarum, a moderately cratered mare surface (figs. 1, 2, and 3). The curve for the lunar uplands was derived from crater counts in the region northwest of crater Tsiolkovskiy, between crater Mendeleev and Mare Smithii. The curve for the southeastern part of Oceanus Procellarum was obtained in an area centered near lat 2°00' N. and long 31°00' W., south of the crater Kunowsky. Oceanus Procellarum has long been considered close to the "average lunar mare" (Hartmann, 1966, 1967); its crater density is intermediate between those of the heavily cratered Mare Tranquillitatis and the lightly cratered Mare Serenitatis.

TABLE 1.—*Crater counts in the Borealis region*

Stratigraphic unit	Counting area (A) (in km²)	Cumulative number (N) of craters (diameter ≥10 km) counted	Number of craters (diameter ≥10 km) per unit area (10^6 km²)	Probable error $\sqrt{N}/A$
Smooth plains material	128,900	12	93	±27
Intermediate plains material	136,800	26	190	±37
Intercrater plains material	236,000	61	258	±30

Material of Borealis Planitia was not included in the smooth plains count because images of the area were blurred by spacecraft motion, and so reliable crater counts could not be obtained. However, smooth plains south of lat 65° N. in the Shakespeare quadrangle, in the crater Strindberg and in Suisei Planitia, are included in these counts. Craters >10 km in diameter that are superposed on the material within the floors of craters Strindberg and Turgenev are included in the plots shown in figure 3.

The plains materials that lie outside Borealis Planitia are distributed in irregular belts, which are subparallel to the terminator and to one another. Eastward from long 190° W., the following belt pattern is observed: intercrater plains material, intermediate plains material, and again intercrater plains material. All three belts extend southward into the Shakespeare quadrangle (Guest and Greeley, 1983).

Distinguishing one type of plains material from another by variations in roughness and crater density is highly dependent on the resolution and lighting conditions of individual Mariner frames (Schaber and McCauley, 1980). This constraint is well documented for the Moon (Masursky and others, 1978, p. 80-81) and for Mars (Boyce and others, 1976). In the Borealis region, where intercrater and intermediate plains materials were imaged at an increasingly low sun angle close to the terminator, the number of observable small craters increase with decreasing distance from the terminator and concomitantly decreasing sun angle. This discrepancy in the apparent abundance of craters occurs only for craters that have small diameters and can be obviated by counting only craters larger than 3 km in diameter.

OLDER PLAINS MATERIALS

The intercrater plains material (unit pi) is the oldest recognizable map unit in the Borealis region. It lies between large craters from about long 155° to long 190° W., and it also occurs between clusters of closely packed and overlapping large craters west of crater Gaugin and south and southeast of crater Mansart. The unit was described originally by Trask and Guest (1975), who considered it to be the most widespread unit on Mercury; Strom (1979) reported that this material covers one-third of the surface viewed by Mariner 10. The principal morphologic characteristic of the intercrater plains material is the high density of superposed craters 5 to 10 km in diameter, which are commonly shallow and elongate; probably they are secondary craters derived from nearby large primary craters that are superposed on the unit. As one group, the large craters and associated intercrater plains form some of the heavily cratered terrain defined by Trask and Guest (1975).

The relative age and nature of intercrater plains material are as uncertain in the Borealis region as they are elsewhere on Mercury. Strom (1979) noted the similarity in surficial morphologies between Mercurian intercrater plains and pre-Imbrian pitted plains south-southwest of Mare Nectaris on the Moon (Wilhelms and McCauley, 1971; Scott, 1972). The pits in the lunar pre-Imbrian pitted plains are similar to the small secondaries that pepper the surface of Mercurian intercrater plains material. On the Moon, pre-Imbrian pitted plains material embays the Janssen Formation (Scott, 1972), whose base is defined as the base of the Nectarian System (Stuart-Alexander and Wilhelms, 1975). However, the crater density of the intercrater plains material in the Borealis region (fig. 1) matches that of an area on the far side of the Moon, in the region northwest of crater Tsiolkovskiy bounded by crater Mendeleev and Mare Smithii. This area is dominated by pre-Nectarian unmantled terra and pre-Nectarian and Nectarian craters (Wilhelms and El-Baz, 1977). The similarity in crater density of intercrater plains material on Mercury and of pre-Nectarian terrain on the Moon is geologically significant, inasmuch as it shows that the oldest recognizable surfaces on both Mercury and the Moon went through similar stages of crustal cratering, but not necessarily at the same absolute geologic time. Differences in crater density as well as embayment relations in the Borealis region show that the intercrater plains material and the smoother intermediate plains material are younger than many c_1 craters in the area northeast of crater Turgenev, and older than smooth plains material in Borealis Planitia.

The relative age of intercrater plains material has a bearing on its origin (Strom, 1979). If very old, intercrater plains material may consist of anorthosite derived from a magma ocean such as may have existed on the Moon (Wood and others, 1970). If emplaced during later stages of Mercurian evolution, it may consist of basin ejecta or lava flows. However, planetwide, the morphologic evidence for an impact origin rather than a volcanic one is not compelling (Strom, 1979). Whether or not either hypothesis is eventually substantiated, the emplacement of intercrater plains material likely began during an early stage of intense accretionary bombardment (Malin, 1976; Guest and O'Donnell, 1977) and lasted until the time of formation of intermediate plains material.

This general conclusion seems to be supported in the Borealis region by the relative scarcity of craters between 30 km and 60 km in diameter (fig. 1). This scarcity may indicate resurfacing by crater overlap and blanketing by crater ejecta or resurfacing by lava flows. Craters ≥60 km in diameter on Mercury also are relatively scarce compared to similar craters in the lunar uplands northwest of crater Tsiolkovskiy (fig. 1). The reduced density of large craters and basins on Mercury relative to the Moon could be either a function of different crater-population rates on these bodies or an effect of different crustal histories (Schaber and others, 1977).

Intermediate plains material (unit psi) has a roughness and crater density transitional between intercrater plains material and smooth plains material (fig. 2). In the Borealis region, the unit occurs in a rather extensive belt that extends from the Shakespeare quadrangle into Borealis north and northeast of Suisei Planitia. Intermediate plains material was first recognized and mapped in the Tolstoj quadrangle (Schaber and McCauley, 1980), where it primarily occurs on the floors of c_1, c_2, and c_3 craters. It was identified there by a lower crater density than that of intercrater plains material and by "a lower incidence of small bright-halo craters than are found on the smooth plains material" (Schaber and McCauley, 1980). Both characteristics are also typical of intermediate plains material in the Borealis region.

BASIN MATERIALS

Goethe Basin is a large circular depression that measures approximately 400 km in diameter from rim crest to rim crest. It was not listed as an impact basin by Wood and Head (1976) because they considered the Mariner 10 photography too poor to confirm basin structures. However, most workers, beginning with Murray and others (1974, p. 174), have identified it as a basin. Goethe is bounded on its north and east sides by a gently sloping wall and discontinuous, low, hummocky rim material that may consist of ejecta deposits. These materials are similar to those occurring around the Caloris Basin in the Tolstoj quadrangle (Schaber and McCauley, 1980). On its west side, Goethe is bounded by at least three subparallel ridges or tilted blocks, which are separated by narrow troughs partly filled with smooth plains material. If an inner concentric ring ever existed (Trask and Strom, 1976), it is buried under the smooth plains material that now extends across the basin. A narrow, concentric structural bench, in part resurfaced by smooth plains material, is recognizable at the base of a gently sloping and much degraded basin wall. Although rectilinear mountain massifs and the radially lineated facies of basin ejecta of the Caloris Group surround the Caloris Basin (McCauley and others, 1981), similar units cannot be unambiguously recognized around the Goethe Basin (FDS 164). However, hilly and hummocky remnants resembling basin deposits and ejecta protrude above the gently sloping basin wall. They extend southwest and north of the basin beyond a much subdued, low, barely perceptible rim crest for a distance of one-half to one-third of the basin radius.

Goethe is older than the smooth plains material by which its wall, rim crest, and most of its ejecta were partly buried. The outlines of the rim crests of several adjacent craters are recognizable through the smooth plains material that partly fills the Goethe Basin (H-1 photomosaic, Davies and others, 1978, p. 28). These buried craters probably were formed on the basin floor after excavation of the basin and were subsequently flooded to their rims by smooth plains material (Strom and others, 1975). The terrain northwest of crater Deprez (FDS 160 and 164) is more hummocky than that farther south, suggesting that smooth plains material northwest of Deprez is so thin that the older and rougher topography of buried intercrater plains material protrudes through it. The density and size of ghost craters within the Goethe Basin are similar to those of the c_2 craters superposed over intercrater plains material near the terminator. These ghost (c_2) craters and the original intercrater plains material they characterize are younger than the Goethe Basin, as they were not obliterated by the impact that formed it. Therefore, Goethe may have impacted onto a surface older than intercrater material and been partly filled by this material at a later date. If so, the Goethe impact basin may be older than some intercrater plains material and large c_1 craters nearby. It is also much older than the Caloris Basin, which was created during the time of formation of c_3 craters (McCauley and others, 1981).

Several additional impact structures within and to the south of the Borealis region display sufficient structural detail to be called basins, even though their diameters are less than the arbitrarily chosen 200-km lower limit adopted by Murray and others (1974) for Mercurian basins. The largest and oldest of these is Botticelli, a crater 140 km in diameter centered at lat 64° N., long 110° W. Only the northernmost parts of the crater's rim and interior lie within the mapped area, but the ghost remnant of an inner ring now flooded by smooth plains material is recognized (FDS 148) farther south in the Shakespeare quadrangle. Turgenev, 110 km in diameter, is large enough to be a central-peak basin (Wood and Head, 1976), even though the peak ring probably has been concealed under smooth plains material. The rims of both Botticelli and Turgenev are covered with densely packed craters, most of which resemble the secondary craters that typically occur on intercrater plains material. Therefore, Botticelli and Turgenev are at least as old as intercrater plains material and may be equivalent in age to the Goethe impact basin. A similar argument can be advanced for the age of the Monteverdi Basin, 130 km in diameter, centered at lat 64° N., long 77° W. in the Victoria quadrangle. The younger craters Jókai and Verdi, which have prominent central peaks and ghostlike discontinuous inner rings, probably qualify as central-peak basins (Wood and Head, 1976). Both structures are considerably younger than the Caloris Basin.

No material similar to either the lineated or the secondary-crater facies of the Van Eyck Formation, the most distinctive and distant unit of the Caloris Group (McCauley and others, 1981), can be unambiguously identified in the Borealis region. A few rounded hills or knobs, too small to be mapped, are present; they are morphologically similar to blocks of the Odin Formation surrounding the Caloris Basin in the Shakespeare quadrangle (Guest and Greeley, 1983), and to features of the Alpes Formation around the Imbrium Basin on the Moon. Two of the most striking of these knobs are possibly 2 km long and 0.2 km across; they rise above smooth plains material that fills a much degraded, unmapped, irregular crater at 69° N., 157° W. (FDS 088). These knobs are about 1,100 km northeast of Caloris Montes and may represent Caloris Basin ejecta. Alternatively, they may be associated with crater Verdi ejecta or with lineated and secondary-crater ejecta that flare southeastward from an unnamed crater north of and adjacent to the crater Nizāmī. Another morphologic feature that may be related to the Caloris Basin event consists of grooves on intercrater plains material and on the southwest-facing walls of craters such as Mansart. These grooves are as much as several kilometers long and several hundred meters wide. The direction of elongation of many small secondary craters also suggests an origin related to the Caloris event.

YOUNGER PLAINS MATERIAL

Smooth plains material (unit ps) forms the vast expanses of Borealis and Suisei Planitiae, as well as most basin and crater floors. It is the most extensive stratigraphic unit in the Borealis region, covering 30 percent of the mapped area. The surface of the smooth plains material is rather sparsely cratered compared to that of the intercrater plains material (figs. 3, 1). Wrinkle ridges are common. Both the floor of the Goethe Basin and the younger craters (now observed as buried craters) superposed on it are mantled by smooth plains material; the unit also fills ghost and flooded craters that are common on both Borealis and Suisei Planitiae and resemble the lunar crater Archimedes. The enormous volume of smooth plains material that must underlie Borealis Planitia in order to bury pre-existing topography, as well as the presence of the material in basin and crater floors, suggest that the smooth plains material was emplaced in a fluidized state as volcanic lava flows (Murray and others, 1974; Strom and others, 1975). Even though flow fronts cannot be unambiguously mapped on Borealis Planitia, further evidence of the units's volcanic origin is supplied by its overlap onto intercrater plains material, best observed along the west edge of Borealis Planitia (FDS 85, 152, 153, 156, and 160).

The various types of plains material recognized on Mercury exhibit little tonal contrast. The albedo of smooth plains material is higher than that of lunar mare material (Hapke and others, 1975). The similarity in albedo between Mercurian smooth plains material and lunar light plains material led Wilhelms (1976) to extend the analogy to composition: he suggested that both units consist of impact ejecta similar to the lunar Cayley Formation sampled by Apollo 16. Wilhelms (1976, p. 556) even hypothesized that the source basin for material of the extensive plains of Borealis Planitia "could well be lurking in the darkness beyond the terminator." A fuller discussion of the problem is given by Strom (1979).

CRATER MATERIALS

In the Borealis region, craters are mapped according to the fivefold classification proposed by McCauley and others (1981), which determines Mercurian crater ages on the basis of crater diameter and morphologic degradation. Craters less than about 30 km in diameter are not mapped. All basins between 100 and 200 km in diameter (including those that have central peaks and peak rings) are mapped as craters. Criteria used to determine impact structures are morphologic crater components such as rays, secondary rays, hummocky rims, various facies of crater ejecta, crater geometry and structure, or a combination of these. The Verdi crater is defined as the type example of a young, large, c_4 crater by McCauley and others (1981), but was mapped as a c_4 crater in the Shakespeare quadrangle (Guest and Greeley, 1983) prior to the release of McCauley and others' crater classification. For this reason, the Verdi crater is also mapped as a c_4 crater in the Borealis region.

No rayed craters >30 km in diameter were observed in the mapped area, but many moderately bright and diffuse rays extend across smooth plains material or occur as halos around very small craters in Borealis Planitia. The most conspicuous of these are indicated on the map. A train of northeast-trending discontinuous rays, which extends across Borealis Planitia as far as the Goethe Basin, may radiate from small unnamed and unmapped rayed craters near the south edge of the map area. The relative scarcity of small bright-halo craters on intermediate plains material, perhaps due to unique physical properties of this material, was first noted in the Tolstoj quadrangle (Schaber and McCauley, 1980); this scarcity is also characteristic of the unit in the Borealis region.

The reduced ballistic range on Mercury compared to the Moon is caused by Mercury's stronger gravitational field (Gault and others, 1975; Strom, 1979; McCauley and others, 1981). This phenomenon, which results in a reduced dispersion of ejecta and secondary craters, is best observed within the Borealis region around craters Verdi (Gault and others, 1975; Trask and Guest, 1975) and Deprez. Slight differences between Mercurian and lunar crater morphologies